

Enhancing Catalytic Performance of Palladium in Gold and Palladium Alloy Nanoparticles for Organic Synthesis Reactions through Visible Light Irradiation at Ambient Temperatures

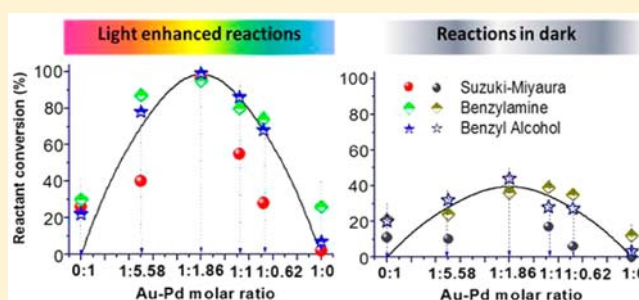
Sarina Sarina,[†] Huaiyong Zhu,^{*,†} Esa Jaatinen,[†] Qi Xiao,[†] Hongwei Liu,[†] Jianfeng Jia,[‡] Chao Chen,[†] and Jian Zhao[†]

[†]School of Chemistry, Physics and Mechanical Engineering, Queensland University of Technology, Brisbane QLD4001, Australia

[‡]School of Chemical and Material Science, Shanxi Normal University, Linfen 041004, China

S Supporting Information

ABSTRACT: The intrinsic catalytic activity of palladium (Pd) is significantly enhanced in gold (Au)-Pd alloy nanoparticles (NPs) under visible light irradiation at ambient temperatures. The alloy NPs strongly absorb light and efficiently enhance the conversion of several reactions, including Suzuki-Miyaura cross coupling, oxidative addition of benzylamine, selective oxidation of aromatic alcohols to corresponding aldehydes and ketones, and phenol oxidation. The Au/Pd molar ratio of the alloy NPs has an important impact on performance of the catalysts since it determines both the electronic heterogeneity and the distribution of Pd sites at the NP surface, with these two factors playing key roles in the catalytic activity. Irradiating with light produces an even more profound enhancement in the catalytic performance of the NPs. For example, the best conversion rate achieved thermally at 30 °C for Suzuki-Miyaura cross coupling was 37% at a Au/Pd ratio of 1:1.86, while under light illumination the yield increased to 96% under the same conditions. The catalytic activity of the alloy NPs depends on the intensity and wavelength of incident light. Light absorption due to the Localized Surface Plasmon Resonance of gold nanocrystals plays an important role in enhancing catalyst performance. We believe that the conduction electrons of the NPs gain the light absorbed energy producing energetic electrons at the surface Pd sites, which enhances the sites' intrinsic catalytic ability. These findings provide useful guidelines for designing efficient catalysts composed of alloys of a plasmonic metal and a catalytically active transition metal for various organic syntheses driven by sunlight.



1. INTRODUCTION

Palladium (Pd) is well-known to be catalytically active for many reactions of important organic syntheses.^{1–3} Many of these reactions are conducted under heating to improve the yield and achieve better reaction efficiency. As thermal enhancement of catalytic performance is energy intensive, it would be a significant breakthrough if we could enhance the catalytic activity of palladium at ambient temperatures using sunlight, the reliable, abundant, and “green” energy source.

While many of the organic synthesis reactions catalyzed by homogeneous Pd catalysts may achieve high yields, it is difficult to recover the catalysts postreaction. We aim to develop efficient, heterogeneous catalysts that function under mild ambient conditions and that can be recovered readily for reuse.

It is well-known that gold nanoparticles (AuNPs) exhibit strong visible-light absorption due to the localized surface plasmon resonance (LSPR),^{4–7} and that they also absorb ultraviolet (UV) light due to interband electron transitions (from 5d to 6sp).^{8–10} The LSPR effect is the collective oscillation of conduction electrons in the NPs, which resonate with the electromagnetic field of the incident light. Through

this process the NPs' conduction electrons gain the irradiation energy resulting in high energy electrons at the surface, which is desirable for activating molecules on the NPs for chemical reactions. Photocatalysts consisting of gold and silver NPs, that function via this mechanism have been developed.^{4–9} The obvious advantage of such a process is that the energy of incident light is very efficiently coupled into the reactant molecules, and not dispersed into the other components of the reaction system, such as the container, solvent and the material that supports the NPs.^{11–13} New catalyst structures could be designed that exploit the vast potential of this process where we use light, instead of heat, as the energy source to drive reactions with unprecedented efficiency.

With this goal in mind, we have incorporated Pd into AuNPs and utilize the engineered properties of the composite alloy NPs to catalyze various reactions with visible light. The catalytic properties of the alloy NP are significantly different from those of pure AuNP or PdNP because of the effect that alloying has

Received: January 16, 2013

Published: March 25, 2013

on the NP's surface electronic properties. Given that the electronegativity of Pd (2.20) is lower than that of Au (2.54) there will be a charge heterogeneity at the alloy NP surface, with both electron-rich sites and slightly positively charged sites present.^{14–17} The electronic heterogeneity means that interactions between the alloy NPs and both electrophilic or nucleophilic reactant molecules can be enhanced.^{18,19} In addition, upon formation of the alloy, electrons will flow across the Au and Pd interface until the electron chemical potential equalizes throughout the alloy NP. Then when the NP is irradiated with light, additional electrons energized through light absorption are also transported since they can remain in an excited “hot” state for up to 0.5–1 ps.^{8,20} This results in energetic electrons collecting at the Pd sites on the NP surface. Thus, it is reasonable to expect that under visible and UV irradiation the Pd sites with the energetic electrons at the alloy NPs surface will exhibit superior catalytic activity to that of pure palladium NPs alone. This significant enhancement of the intrinsic catalytic activity of palladium makes it possible to apply the alloy NP catalysts to drive various reactions at ambient temperatures with light.

In the present study, several organic reactions were studied for confirming the general applicability of Au–Pd alloy NP catalysts for various reactions under visible light irradiation. Suzuki–Miyaura cross-coupling is a widely used reaction for the formation of C–C bonds,^{2,21,22} and oxidative addition of benzylamine is an effective route to produce imine (C–N coupling).^{23–25} Imine derivatives are important building blocks for the synthesis of fine chemicals and pharmaceuticals,^{26,27} and the strategy for the direct oxidation of amines has attracted much interest.^{25,28–30} Selective (partial) oxidation of aromatic alcohols to the corresponding aldehydes or ketones with O₂ is also a class of fundamental reactions for organic synthesis.³¹ The product carbonyl compounds can serve as important and versatile intermediates for fine chemicals synthesis.^{32–35} In catalyzing these reactions, we found that the alloy NPs outperformed pure NPs of Au and Pd and that, in addition, when irradiated with visible light the performance of the alloy NPs was significantly enhanced.

2. METHODS

Catalyst Preparation. Catalysts with 3 wt % of pure gold NPs on ZrO₂ (labeled 3%Au), 3 wt % of pure Pd NPs on ZrO₂ (3%Pd) and three catalysts of Au and Pd alloy NPs supported by ZrO₂ (abbreviated Au–Pd@ZrO₂), with different Au/Pd ratios were prepared by impregnation–reduction method. For example, 1.5 wt %Au–1.5 wt % Pd/ZrO₂ was prepared by the following procedure: 2.0 g ZrO₂ powder was dispersed into 15.2 mL of 0.01 M HAuCl₄ aqueous solution and 28.3 mL of 0.01 M PdCl₂ aqueous solution were added while magnetically stirring. A total of 20 mL of 0.53 M lysine was then added into the mixture with vigorous stirring for 30 min. To this suspension, 10 mL of 0.35 M NaBH₄ solution was added dropwise in 20 min, followed by an addition of 10 mL of 0.3 M hydrochloric acid. The mixture was aged for 24 h and then the solid was separated, washed with water and ethanol, and dried at 60 °C. The dried solid was used directly as catalyst. Catalysts with other Au/Pd ratios were prepared in a similar method but using different quantities of HAuCl₄ aqueous solution or PdCl₂ aqueous solution.

Catalyst Characterization. A TEM study and line profile analysis by the energy dispersion X-ray spectrum technique carried out on a Philips CM200 TEM with an accelerating voltage of 200 kV were used to characterize the catalysts. The Au and Pd content of the prepared catalysts were determined by EDX technology using the attachment to a FEI Quanta 200 Environmental SEM. The element line scanning was conducted on a Bruker EDX scanner attached to JEOL-2200FS TEM

with scanning beam diameter down to 1.0 nm. X-ray diffraction (XRD) patterns of the sample powders were collected using a Philips PANalytical X'pert Pro diffractometer. CuK α radiation ($\lambda = 1.5418 \text{ \AA}$) and a fixed power source (40 kV and 40 mA) were used. DR-UV–vis spectra of the sample powders were examined by a Varian Cary 5000 spectrometer.

Activity Test. The suspension of catalyst powder, solvent and the reactant was placed in a chamber in which a 500 W Halogen lamp (from Nelson, wavelength in the range 400–750 nm) was used as a light source and the light intensity was usually 0.30 W/cm² (except for the experiments investigating the impact of the intensity). The temperature of the reaction system was carefully controlled with an air-conditioner attached to the chamber. The reaction system under light illumination was maintained at the same temperature as the corresponding reaction system in the dark to ensure that the comparison is meaningful. The details of the reaction systems are given briefly as footnotes of Table 1 for each reaction. At given irradiation time intervals, 2 mL aliquots were collected, centrifuged, and then filtered through a Millipore filter (pore size 0.45 μm) to remove the catalyst particulates. The filtrates were analyzed by gas chromatography (HP6890 Agilent Technologies) with a HP-5 column to measure the concentration change of reactants and products.

3. RESULTS AND DISCUSSION

Transmission electron microscopy (TEM) analysis of the alloy NPs (Figure 1A–C) shows that the mean diameters of the Au–Pd alloy NPs are less than 8 nm (Figure 1B). Figure 1D is a line profile analysis of the energy dispersion X-ray (EDX) spectrum for a typical Au–Pd alloy NP in Figure 1A, showing that the NP consists of both Au and Pd distributed spherically around a common center, which means that the two metals exist as binary alloy NPs in this sample.

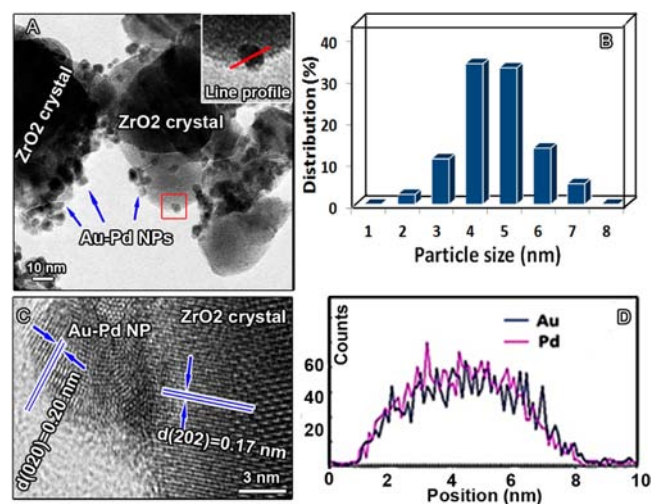


Figure 1. (A) TEM image of Au–Pd@ZrO₂ catalyst. The arrows indicate Au–Pd NPs. (B) Particle size distribution of Au–Pd@ZrO₂ used in this study. (C) High resolution TEM images of an alloy particle in catalyst. (D) The line profile analysis of EDX spectra for a typical Au–Pd NP indicated by the red square and the inset in (A), providing the information of the elemental composition and distribution of the NP.

Evidence of the formation of Au–Pd alloy NPs is seen in the observed light absorption of the sample as shown in Figure 2. Here, the spectrum of the Au–Pd alloy NPs sample is clearly different from the spectra of the pure metal NPs. This is believed to be associated with the formation of Au–Pd alloy NPs.^{36–38} ZrO₂ has a band gap of about 5 eV³⁹ and exhibits weak visible light absorption at wavelengths above 400 nm, and

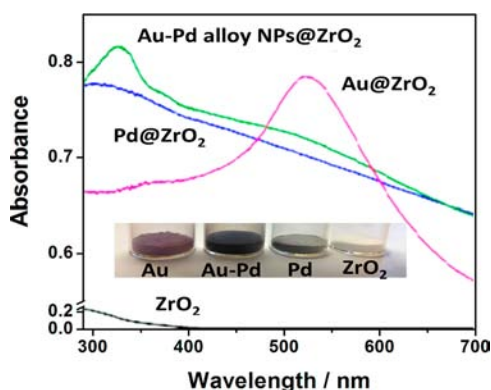


Figure 2. Diffuse reflectance UV–visible (DR-UV–vis) spectra of the Au–Pd@ZrO₂ catalyst and their comparison with pure Au@ZrO₂ and Pd@ZrO₂. The inset is a photograph of the catalysts.

therefore, the ZrO₂ support itself does not contribute to photocatalytic activity. In contrast, all the Au, Pd, and Au–Pd alloy catalysts on the ZrO₂ supports, display high levels of absorption in the UV and visible range, indicating that solar energy is strongly coupled to the metal NPs. The absorption peak at 520 nm in the spectrum of the pure AuNP sample corresponds to the LSPR of the AuNPs.^{4–7} The presence of the support and its interaction with the AuNPs can shift and broaden this peak. The AuNPs also absorb UV irradiation through interband (*Sd* → *6sp*) transitions.^{8–10} The LSPR for the pure PdNPs is deep within the UV region so its light absorption at solar wavelengths occurs through both LSPR and interband electron transition contributions.

Table 1 shows the results of light-enhanced reactions using the Au–Pd@ZrO₂ catalyst with an optimal Au/Pd molar ratio

of 1:1.86. The results of reactions in the dark at same temperature and performance of Au@ZrO₂ and Pd@ZrO₂ catalysts are also provided for comparison. The overall metal content in the three catalysts was the same being 3 wt % of the catalyst. As can be seen in Table 1, the irradiation increased the product yield of the Suzuki coupling at 30 °C to 96% (from 37% in the dark), and the yield of oxidation of benzylamine at 45 °C to 95% (from 36% in the dark at 45 °C), and the yield of selective oxidation of benzyl alcohol to 99% (from 44% in dark at 45 °C). Control experiments using ZrO₂ (without Au–Pd alloy NPs) as the catalyst were performed. No conversion was observed for the reaction when the system was illuminated with incident light nor when the reaction was allowed to proceed in the dark. This confirms that the catalytic activity is due to the Au–Pd alloy NPs and that the catalytic enhancement observed when the system was irradiated with light is also caused by the NPs. These results indicate that the Au–Pd alloy NPs function as photocatalysts and that under visible light irradiation the catalytic performance of palladium for these organic synthesis reactions at ambient temperatures is significantly enhanced. The data obtained from the three reactions will be discussed in more detail later.

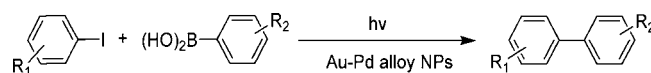
The results in Table 1 show an interesting trend. For reactions conducted in the dark where the PdNPs exhibit substantial activity and the AuNPs showed some, albeit lower, activity, such as the first four reactions in Table 1, the Au–Pd alloy NPs exhibited superior photocatalytic activity to both the AuNPs and the PdNPs. However, for reactions that pure AuNPs exhibit significant activity but PdNPs do not, such as the last two reactions in Table 1, the photocatalytic performance of the Au–Pd alloy NPs was inferior to that observed for the pure AuNPs. Thus, for this second class of

Table 1. Performance of the Catalysts of Au–Pd Alloy NPs, Pure AuNPs, and Pure PdNPs Supported on ZrO₂ for Different Types of Reactions^a

Reaction	Light	Product Yield / %		
		Au	Au-Pd alloy	Pd
1 Suzuki-Miyaura cross-coupling (Positive alloy effect)	Visible	2	96	26
	Dark	0	37	11
2 Oxidation of benzylamine into imines (Positive alloy effect)	Visible	26	95	30
	Dark	12	36	21
3 Selective oxidation of aromatic alcohols (Positive alloy effect)	Visible	7	100	22
	Dark	3	44	20
4 Phenol degradation (Positive alloy effect)	Visible	0	31	14
	Dark	0	11	10
5 Hydroamination of alkyne (Negative alloy effect)	Visible	45	0	0
	Dark	15	0	0
6 Reduction of nitrobenzene to azobenzene (Negative alloy effect)	Visible	100	54	0
	Dark	0	0	0

^aThe data of the reaction in the dark at the same temperature is provided for comparison. The detailed data, including turnover number, turnover frequency, and quantum yield, are given in Tables 2–4.

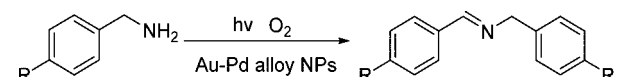
Table 2. Suzuki-Miyaura Cross-Coupling Reactions Catalyzed with the Au–Pd@ZrO₂ Catalysts of Various Au/Pd Molar Ratios under Visible Light Irradiation (Numbers in Red Color) and in the Dark (Numbers in Black Color)^a



R ₁	R ₂	Au:Pd ^[a]	Yield / %		Selec. / %		TON		TOF / h ⁻¹		Q.Y. / %
			Light	Dark	Light	Dark	Light	Dark	Light	Dark	
3-CH ₃	4-H	1:1.86	96 ^[b]	37	99	99	87	34	14.5	5.7	2.7
		1:1.00	55 ^[b]	17	98	99	56	17	9.3	2.8	1.7
		1:5.58	40 ^[b]	10	99	99	34	8	5.7	1.3	1.4
		1:0.62	28 ^[b]	6	99	100	33	6	5.5	1.0	1.0
		1:0	2 ^[b]	0	100	---	3	0	0.5	0	0.1
4-CH ₃	4-H	1:1.86	94 ^[b]	46	98	97	95	46	15.8	7.7	2.2
		1:1.86	86 ^[b]	30	98	98	87	30	14.5	5.0	2.6
		1:1.86	96 ^[c]	41	98	99	97	41	19.4	8.2	2.5
		1:1.86	99 ^[d]	58	99	99	100	99	50.0	0.0	1.9
		1:1.86	98 ^[e]	65	99	96	99	67	24.8	0.0	1.5
4-H	4-N(CH ₃) ₂	1:1.86	80 ^[f]	55	68	60	81	56	3.0	0.0	0.3

^a[a] Molar ratio; [b] Reaction time 6 h; [c] Reaction time 5 h; [d] Reaction time 2 h; [e] Reaction time 4 h; [f] Reaction time 22 h. Reaction conditions: 1 mmol of aryl iodide, 1.5 mmol of aryl boronic acid, 50 mg (containing 3% of metals) of catalyst and 3 mmol of base K₂CO₃ in DMF/H₂O = 3:1 (solvent) at 30 °C and 1 atm of argon. TON and TOF were calculated based the total amount of metal(s). The calculation method of quantum yield (Q.Y.) is given in Supporting Information (SI).

Table 3. Catalytic Oxidation of Benzylamine into Imines with the Au–Pd@ZrO₂ Photocatalysts of Various Au/Pd Molar Ratios under Visible Light Irradiation (Number in Red Color) and in the Dark (Number in Black Color)^a



R	Au:Pd ^[a]	Yield / %		Selec. / %		TON		TOF / h ⁻¹		Q.Y. / %
		Light	Dark	Light	Dark	Light	Dark	Light	Dark	
H	1:1.86	95 ^[b]	36	96	98	86	33	0.90	0.34	2.7
	1:1.00	84 ^[b]	39	99	98	91	39	0.95	0.41	1.7
	1:5.58	80 ^[b]	24	95	96	75	21	0.78	0.22	1.4
	1:0.62	74 ^[b]	35	99	98	86	41	0.90	0.43	1.0
	1:0	26 ^[b]	12	97	98	34	16	0.35	0.17	0.1
	0:1	30 ^[b]	21	89	83	21	15	0.22	0.16	0.7
Cl	1:1.86	98 ^[c]	16	93	99	89	18	2.23	0.45	2.2
CH ₃	1:1.86	33 ^[d]	11	100	100	40	15	0.83	0.31	2.6
OCH ₃	1:1.86	43 ^[d]	15	98	99	44	16	0.92	0.33	2.5

^a[a] Molar ratio; [b] Reaction time 96 h; [c] Reaction time 40 h; [d] Reaction time 48 h. Reaction conditions: 1 mmol of reactant, 50 mg (containing 3% of metals) of catalyst in CH₃CN solvent at 45 °C and 1 atm of O₂. TON and TOF were calculated based the total amount of metal(s). The calculation method of Q.Y. is given in SI.

reactions, where the catalytic activity is Au dominated, the Au–Pd alloy NPs did not perform better than the mono metal NPs. These results imply that, in reactions where the catalytic activity is Pd dominated, the intrinsic catalytic activity of palladium is significantly enhanced in the alloy NPs by light irradiation, even when at ambient temperatures. This provides a general guiding principle for determining under what conditions that light-enhanced performance of alloy NP catalysts can be expected as well as providing design criteria for selecting transition metals to alloy with gold to catalyze specific reactions with light driven processes. These concepts will be demonstrated in the following discussion.

PdNPs are not effective catalysts in the hydroamination of alkyne or the reduction of nitrobenzene to azobenzene (entries 5 and 6 in Table 1). Because the catalytically active sites for these two reactions are not the Pd sites at the surface, it is not expected that the photocatalytic performance of the alloy NP would be any better than that of AuNPs. The significant role that the Pd sites at the external surface of the alloy NPs play in some of the catalytic processes, such as the selective oxidation of benzyl alcohol, was demonstrated by preparing a sample of NPs with a Pd core and an Au shell by reducing HAuCl₄ on a Pd–ZrO₂ support with H₂. This sample has almost no Pd sites at the NP surface and exhibited low activity for selective

Table 4. Catalytic Oxidation of Aromatic Alcohols with the Au–Pd@ZrO₂ Catalysts of Various Au/Pd Molar Ratios under Visible Light Irradiation (Number in Red Color) and in the Dark (Number in Black Color)^a

Reactant	Au:Pd ^[a]	Yield / %		Selec. / %		TON		TOF / h ⁻¹		Q.Y. / %
		Light	Dark	Light	Dark	Light	Dark	Light	Dark	
Benzyl alcohol	1:1.86	100 ^[b]	44	99	100	114	51	22.8	10.2	5.2
	1:1.00	89 ^[b]	28	98	98	91	35	18.2	7.0	5.6
	1:5.58	78 ^[b]	32	96	98	62	37	12.4	7.4	4.2
	1:0.62	68 ^[b]	27	99	100	78	51	15.6	10.2	3.8
	1:0	7 ^[b]	3	100	100	9	4	1.8	0.8	0.3
	0:1	22 ^[b]	20	99	99	15	14	3.0	2.8	0.2
4-Methylbenzyl alcohol	1:1.86	95 ^[c]	44	93	97	115	61	28.8	15.3	4.7
	1:0	21 ^[c]	11	99	98	28	15	7.0	3.8	0.9
	0:1	19 ^[c]	13	98	96	14	9	3.5	2.3	0.5
4-Methoxybenzyl alcohol	1:1.86	100 ^[d]	56	94	96	115	47	57.5	23.5	4.0
	1:0	26 ^[d]	10	98	99	34	13	17.0	6.5	1.5
	0:1	29 ^[d]	22	92	96	21	15	10.5	7.5	0.7
1-Phenylethanol	1:1.86	98 ^[e]	31	95	99	115	30	19.2	5.0	6.2
	1:0	11 ^[e]	6	100	100	15	8	2.5	1.3	0.5
	0:1	25 ^[e]	26	96	97	18	19	3.0	3.2	0
Cinnamyl alcohol	1:1.86	100 ^[f]	62	91	93	101	58	5.1	2.9	8.1
	1:0	30 ^[f]	22	89	94	40	29	2.0	1.5	5.2
	0:1	47 ^[f]	32	88	89	33	23	1.7	1.2	5.6

^a[a] Molar ratio; [b] Reaction time 5 h; [c] Reaction time 4 h; [d] Reaction time 2 h; [e] Reaction time 20 h; [f] Reaction time 22 h. Reaction conditions: 2 mmol of the reactant, 50 mg (containing 3% of metals) of catalyst in trifluorotoluene solvent at 45 °C and 1 atm of O₂. TON and TOF were calculated based the total amount of metal(s).

oxidation of benzyl alcohol (10% conversion compared to 100% achieved by the Au–Pd alloy NP).

We also found that the performance of the Au–Pd@ZrO₂ catalysts strongly depends on the Au/Pd molar ratio for the first three reactions in Table 1 both in the presence and absence of light. The detailed data of the three reactions, Suzuki–Miyaura cross-coupling, oxidative addition of benzylamine, and selective oxidation of aromatic alcohols, are provided in Tables 2–4.

There are many reports on the Suzuki–Miyaura coupling reactions via homogeneous catalytic processes catalyzed by palladium complexes with various ligands. With these homogeneous catalytic processes it is difficult to recycle the catalyst, which is an important consideration from an industrial application perspective and in minimizing the impact on the environment.⁴⁰ The Suzuki–Miyaura coupling can also be catalyzed by heterogeneous catalysts of the supported PdNPs, but all of them are at elevated temperatures (≥ 60 °C). For example, PdNPs on mesoporous silica MCM41 achieved a yield of 93% at 78 °C after 5 h. When the NPs were supported on carbon nanotubes, the yield was 87–94% at 70–100 °C. A table summarizing the various reaction conditions previously considered and details of the catalyst used are provided in SI (Table S1). This table shows that the Au–Pd alloy NP catalysts under investigation here can drive the same reactions at much lower temperatures (only 30 °C) under visible light irradiation while still achieving excellent yields. This means that by alloying with Au, we introduce light, which enhances the performance of Pd catalyst for synthesis reactions.

Generally, the synthesis of imine derivatives involves condensation of an amine and a carbonyl compound. To solve the problem caused by the excessively active nature of ketones or aldehydes, an alternative strategy to the direct oxidation of amines has attracted much interest.^{25,28–30,41} Ruthenium based catalysts have been developed for this purpose,⁴² but they oxidize only a limited range of amines into imines at relatively high temperature (mostly >110 °C). A. Grirrane et al. reported 5% Pd/TiO₂ catalyst can oxidize benzylamine at 100 °C temperature and 5 atm O₂ pressure, with a product yield that may reach 75% after 30 h (5% Au/TiO₂ and Pt/TiO₂ show catalytic activity under the same reaction conditions and reaction time with product yields of 98% and 22%).²⁸ Photocatalytic processes with carbon nitride (graphitic, C₃N₄) for oxidative coupling of benzylamine were revealed by F. Su et al., with the reactions taking place under 5 atm O₂ pressure at 60–80 °C with visible light irradiation. These high reaction temperatures and pressure indicate that this reaction requires critical conditions when using supported noble metal nanoparticle as the catalyst. The most moderate reaction conditions reported for this reaction so far is the UV light photocatalytic oxidation of amines with TiO₂.⁴³ However, the UV light irradiation may result in a relatively lower product selectivity.

The first successful example of palladium-catalyzed aerobic oxidation of alcohols was reported by Blackburn and Schwartz in 1977,⁴⁴ however, only a few heterogeneous catalysts of supported PdNPs and Pd^{II} species are available to date. For example, Pd on hydrotalcite,^{45,46} carbon,^{45,47} Al₂O₃,⁴⁵ SiO₂,⁴⁵ pumice,⁴⁸ SiO₂–Al₂O₃ mixed oxide,⁴⁹ TiO₂,⁵⁰ and polymer-

supported Pd.⁵¹ As shown in Table S2 (in SI), those catalysts, both in the metallic NPs or immobilized ionic state, can catalyze the benzyl alcohol oxidation at elevated temperatures and high pressure. The process with PdNPs on hydrotalcite achieved a yield of 99% in an hour at 90 °C. Au–Pd alloy NPs supported on TiO₂ were also used as the catalyst of this reaction, which exhibited improved catalytic activity (a yield $\leq 70\%$ in 8 h), compared to PdNPs, but at a higher temperature (100 °C) and pressure (2 atm O₂). The lower yield could be attributed to the lower stability of the product, benzaldehyde, at higher temperatures and pressures. The selective oxidation with O₂ is an exothermic reaction. Hence, the photocatalytic process at low reaction temperatures proposed in the present study is thermodynamically preferred. Utilizing light energy to promote the efficiency of this process requires low energy input.

The results in Tables 1–4 show that, without light irradiation, pure AuNPs exhibit no catalytic activity for Suzuki–Miyaura cross-coupling, a low activity (with a yield of 12%) for the oxidation of benzylamine into imine, and very low activity (yield of 3%) for the oxidation of benzyl alcohol. The activity of the pure PdNPs for these three reactions are better than those observed with AuNPs, but still relatively low (yields are between 11 and 21%). The alloy NPs exhibited improved activity for the reactions in the dark. For example, for the three reactions, the yields achieved with the alloy NPs with the optimal Au/Pd ratio of 1:1.86 are between 36 and 44%. The underlying cause of this dependence on alloy composition has not been fully understood, yet. We note that the optimal Au: Pd molar ratio for the Au–Pd alloy NP catalysts used for reactions at high temperature (≥ 190 °C) and high pressure, reported by other groups,^{52,53} is similar to that in the present study.

Visible light irradiation of the alloy NP catalysts significantly increased the yields of the reactions (up to 95 and 100%). It enhances the conversion rate of the reactions while it has little impact on the product selectivity (see Tables 2–4).

To better understand the enhancement of the catalytic performance that occurs through light irradiation of the Au–Pd alloy NPs, the dependence of the catalyzed reaction on the light's wavelength and intensity were investigated. The specific example of Suzuki–Miyaura coupling is used with the results shown in Figures 3 and 4.

As shown in Figure 3, increasing the light intensity resulted in an almost linear increase in the conversion of the Suzuki–Miyaura coupling reaction catalyzed by the Au–Pd alloy NPs.

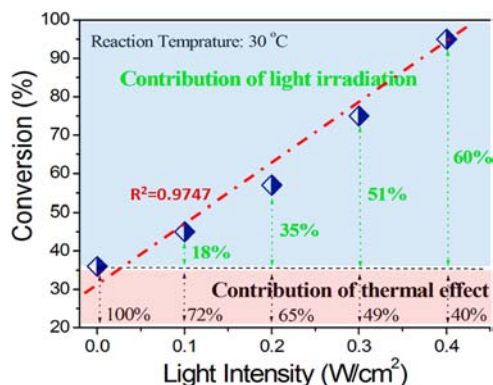


Figure 3. The dependence of the catalytic activity of Au–Pd alloy NPs for the Suzuki–Miyaura coupling reaction on the intensity of the light irradiation. Both light driven reaction and the reaction in the dark were conducted at 30 ± 1 °C.

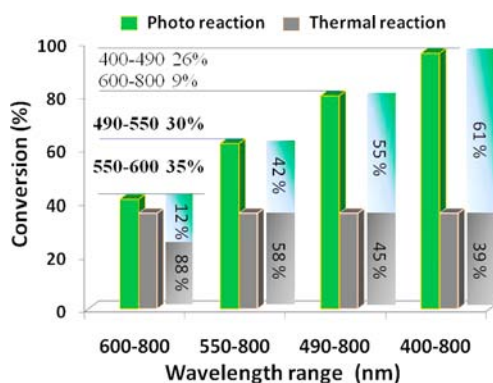


Figure 4. Dependence of the catalytic activity of Au–Pd alloy NPs for the Suzuki–Miyaura coupling reaction on the wavelength of the light irradiation. Both light driven reaction and the reaction in the dark were conducted at 30 ± 1 °C.

To ensure that thermal effects could be discounted, the temperature of the reaction mixture was carefully controlled and maintained at $30 \text{ °C} \pm 1 \text{ °C}$. The contribution of the conversion efficiency that can be attributed to light irradiation was calculated by subtracting the conversion efficiency of the reaction in the dark from that observed when the system was irradiated, with both reactions occurring at same temperature. Here the conversion efficiency observed in the absence of light is the thermal contribution. The relative contributions of light and thermal processes to the conversion efficiencies are shown in Figure 3. It can be seen, the higher the light intensity, the greater the contribution due to light irradiation to the overall conversion rate. For example, when the light intensity is 0.2 W/cm^2 , only 35% of the conversion results from light irradiation with 65% attributed to the thermal effects at $30 \text{ °C} \pm 1 \text{ °C}$. When the light intensity is 0.4 W/cm^2 , 60% of the conversion is due to light irradiation. For the selective oxidation of benzyl alcohol, the contribution attributed to light irradiation also increased from 24% at 0.1 W/cm^2 to 36, 49, and 56% at 0.2, 0.3, and 0.4 W/cm^2 (Figure S2 in SI). This trend clearly demonstrates the enhancement that light irradiation produces in the catalytic activity of Au–Pd alloy NPs.

To determine the effect on the conversion efficiency that the wavelength of the light used to irradiate the systems has, we used various optical low pass filters to block light below specific cutoff wavelengths. Thus, we could tune the wavelength range that irradiated the reaction systems. The dependence of the catalytic performance on wavelength range for the Suzuki coupling reaction is illustrated in Figure 4 and the results for benzyl alcohol oxidation are provided in Supporting Information as Figure S3.

Without any filters, light with wavelengths between 400–800 nm illuminated the system and a conversion efficiency of 95% was observed. Applying a filter that transmitted wavelengths in between 490–800 nm saw the conversion efficiency decrease to 80%. When the light was filtered so that only wavelengths between 550–800 nm were transmitted the conversion dropped to 62%, while filtering the incident light to transmit wavelengths between 600–800 nm saw the conversion decrease further to 41%. Given that the reaction conversion in the dark at this temperature was 37%, irradiating the system with light that has wavelengths longer than 600 nm produces little change ($4\% = 41 - 37$) to the reaction. In contrast the contribution from the light with wavelengths in the range of 400–600 nm is 55% ($= 96 - 41$), accounting for 57% of the total conversion

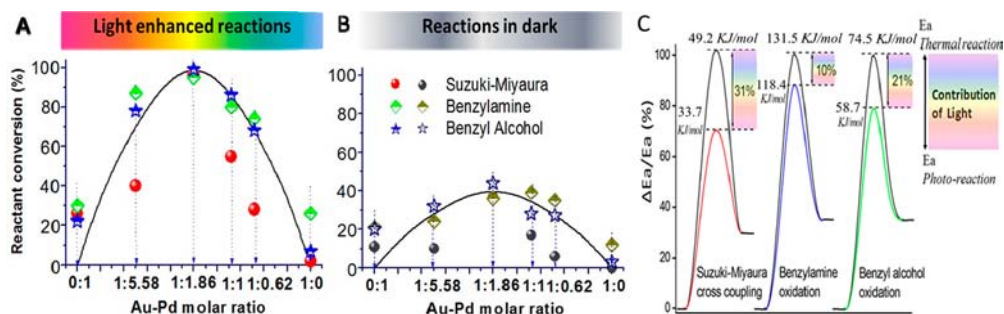


Figure 5. Dependence of Au–Pd@ZrO₂ performance on the Au/Pd molar ratio of the alloy NPs in light-enhanced reaction (A) and in the dark reaction (B) for the three reactions in the present study. (C) Apparent activation energies of the reactions are calculated for the visible-light-enhanced reaction and the reaction in the dark, contribution of light irradiation is calculated from difference of conversion of two processes (with and without light) and presented by percentage.

rate ($55/96 \times 100\%$) and over 91% of the contribution from visible light irradiation [$54/(96-37) \times 100\%$]. Similarly, we can calculate the contribution to the conversion efficiency for any of the specific wavelength ranges used. As illustrated in Figure 4, light in the wavelength ranges 490–550 nm and 550–600 nm account for 30 and 35%, respectively, of the light-induced conversion (conversion difference of visible-light-enhanced reaction and the reaction in the dark), while light in the wavelength ranges of 400–490 nm and 600–800 nm contribute the remaining 35%.

Similarly, in the selective oxidation of benzyl alcohol, irradiation with light with wavelengths between 490–550 (32%) and 550–600 nm (34%) has the largest effect on conversion efficiency, while light at other wavelengths ranges produces the remaining 34% of light-induced conversion (Figure S2 in SI). A common feature for these light-enhanced reactions is that the largest contribution to the catalytic performance results from radiation with wavelengths between 490 and 600 nm (>64%). The energy absorbed by the NPs from light in this wavelength range was estimated from the overlap of the absorption spectrum of the Au–Pd alloy NPs with the spectral irradiance of incandescent light used (Figure S4 in SI), to be 36.2% of the total light energy absorbed by the NPs. Given that the LSPR peak of AuNPs is in this wavelength range, these results suggest that the gold in the alloy NPs functions as an antenna for visible light absorption.

It was also found that the wavelength range producing the largest performance enhancement with the Au–Pd alloy NPs (490–600 nm) is broader than that displayed by AuNPs. In our recent study on selective reactions catalyzed by AuNPs illuminated with visible light (acetophenone hydrogenation to 1-phenyl ethyl alcohol and styrene oxide reduction to styrene),^{54,55} light in the wavelength range 490 to 550 nm was found to provide the main contribution that drove these reactions, as shown in Figure S4 in SI. The light-induced contributions attributed to this wavelength range for the two reactions were 41 and 65%, respectively. The contribution of light in the wavelength range of 550–600 nm was much less (24 and 0%). While for the Au–Pd alloy NPs described in this present study, the contribution of light with wavelengths in the range 550–600 nm is much more significant. This observation confirms that Au–Pd alloy NPs have the potential to utilize visible light energy from broader portion of the spectrum than AuNPs in light-enhanced reactions.

The dependence of the catalytic performance of three light-enhanced reactions on Au/Pd molar ratio of the alloy NPs is illustrated in Figure 5A based on the data of Tables 2–4, while

the observations of the same reactions performed in the dark are shown in Figure 5B for comparison. All three reactions achieved the highest yield of target products when the molar ratio was 1:1.86. Alloy NPs with other Au/Pd ratios (1:5.58, 1:1 and 1:0.62) proved less active. Interestingly, the dependence on the Au/Pd ratio of the alloy NPs for the reactions in the dark is similar to that observed for the light-enhanced reactions but with much lower conversion efficiencies. The figure shows while light illumination and alloy composition both impact on catalytic performance of the alloy NPs, that irradiation with light has a more pronounced effect than the Au/Pd ratio.

A comparison between the contributions to catalytic performance of light irradiation and the alloy component ratio of Au and Pd was performed. We define the contribution of ratio (CoR) as the difference between the conversion rates of thermal reactions undertaken without light when catalyzed by alloy NPs with different Au/Pd ratios; and the contribution of light irradiation (CoL) as the increase in the conversion rate from that observed in the dark when the incident light is introduced. For the Suzuki-Miyaura coupling (Table 2), the CoR calculated between any two Au/Pd ratios is in the range of 4 to ~31%, while the CoL is in the range of 22 to ~59%, which indicates that the light irradiation enhances the catalytic activity for this reaction more significantly than the component ratio. For the other two reactions (Tables 3 and 4), this trend is even more significant: CoRs of the benzylamine oxidation and benzyl alcohol oxidation are in the ranges 1 to ~15% and 1 to ~17%, respectively, which are much lower than the CoLs of 39 to ~59% and 41 to ~61%. These results demonstrate that a greater improvement in the catalytic performance of Au–Pd alloy NPs is obtained with light irradiation than by varying the alloy component ratio.

One possible explanation for these observations is that the charge heterogeneity at the alloy NPs' surface results in the improved catalytic activity of the alloy structure,^{15–17} as the dependence of the performance on the ratio was observed in reactions in the dark with a similar trend to that observed with the light driven reactions (Figure 5A,B). At the Au/Pd ratio of 1:1.86, the surface charge heterogeneity is optimal for the catalysis both in the presence and absence of light. To further confirm the charge heterogeneity at the surface of the alloy NPs, simulations using the density function theory (DFT) were carried out for electron states with and without light irradiation; the wavelength of the light is chosen around the SPR absorption of Au in Figure 2 (530 and 535 nm). Calculation capacity limitations of our DFT simulation necessitated the examination of a small gold cluster Au₃₂ and an alloy cluster

Au₁₂Pd₂₀ as a first step. The charge heterogeneity, indicated by the natural charge distributions, of the two clusters in the ground state (corresponding to the state in the dark) and an excited state (corresponding to that under light irradiation) were simulated. The detailed calculation method and the calculated natural charge distributions are given in SI (TextS2). The results of the calculation confirm that a charge heterogeneity exists even in the pure gold Au₃₂ clusters and that alloying increases the charge heterogeneity of the Au₁₂Pd₂₀ cluster surface (Figure S5 in SI). This charge heterogeneity is to be expected and in agreement with previous reports.^{14,56} When the alloy cluster is irradiated with light, the conduction electrons absorb energy, raising the cluster into one of the excited states. Interestingly for both clusters, the calculated natural charge distribution for the excited state is similar to that calculated for the ground state. Because the charge distribution of the cluster and, therefore, the charge heterogeneity, is strongly influenced by the Au/Pd ratio, changing this ratio will alter the charge distributions of ground and excited states in a more or less similar manner. By extension, varying the Au/Pd ratio will produce the same trend in the catalytic performance of the Au–Pd@ZrO₂ alloy NPs, regardless of whether the reaction system is irradiated with light or in the dark. The increased charge heterogeneity means that interactions between the alloy NPs and reactant molecules is enhanced.^{12,13} There is a much higher probability that the reactant molecules are adsorbed on the alloy NPs than on AuNPs. When the alloy NPs are irradiated with light, the conduction electrons are elevated into excited states through absorption of light energy increasing the NPs capability of inducing reactions involving the adsorbed reactant molecules, over that seen when the same reaction is performed in the dark.

Utilizing this knowledge and information from literature, we propose reaction pathways for three reaction processes that use the Au–Pd@ZrO₂ photocatalyst. The first key step of Suzuki–Miyaura coupling is the activation of iodobenzene on the electron-rich Pd sites at the surface of Au–Pd alloy NPs (as illustrated in S1A in SI), which is made possible because of the intrinsic catalytic activity of palladium to Suzuki–Miyaura coupling.^{40,57} Following on from this, the aromatic borate species react with the activated aryl species from the aryl iodide on the electron-rich surface Pd sites (so-called transmetalation). The final step is reductive elimination of the cross-coupling product R₁Ph–PhR₂ molecule, which returns the initial alloy surface, completing the photocatalysis cycle. Light irradiation significantly enhances the surface charge heterogeneity, which subsequently increases the interaction (absorption of reactant molecule on NP surface) between reactant molecules and Au–Pd alloy NPs. This then results in a higher catalytic activity when the system is irradiated with light than when it is in the dark.

For the process of oxidative coupling of benzylamine into imines (shown in Scheme S1B), the most probable mechanism is that benzylamine is first oxidized into benzaldehyde by abstraction of α -H from the –CH₂– group, followed by the nucleophilic attack of these nascent aldehydes by the unreacted amines to yield the corresponding imines.^{23,24} The abstraction of α -H from the –CH₂– group and formation of alloy-H species also take place in the first step of the pathway for the selective oxidation of aromatic alcohols to the corresponding aldehydes or ketones,^{58,59} as shown in Scheme S1C. The dehydrogenated species then undergo a C–H bond cleavage, yielding aldehyde or ketone as the product.

We calculated the apparent activation energy of the reaction under light irradiation and in the dark by applying the Arrhenius equation and using the reaction data taken at several temperatures, dependent on the reaction, in the range of 30 to 70 °C. For each reaction, the difference between the activation energies of the light-enhanced process and the process in the dark (ΔE_a) indicates the contribution due to light irradiation in reducing the apparent activation energy.⁵⁴ For example, as illustrated in Figure 5C, the apparent activation energy for the Suzuki–Miyaura coupling in the dark is \sim 49.2 kJ/mol, while it is \sim 33.7 kJ/mol for the reaction under visible light illumination. Visible light irradiation reduces the activation energy of Suzuki–Miyaura coupling by 15.5 kJ/mol, which represents 31% of the activation energy. Similarly, the activation energies of selective oxidation of benzyl alcohol and benzylamine oxidative coupling are reduced by 15.8 and 13.1 kJ/mol, respectively, which means that visible light irradiation reduces the apparent activation energy of these two reactions by 21 and 10%, respectively.

The apparent quantum yield of the reactions with the Au–Pd@ZrO₂ catalysts when illuminated with visible light were estimated by subtracting the conversion rate of a reaction performed in the dark from that observed when the system was irradiated with light and performed at the same temperature. The yields are 2.7, 3.8, and 8.1%, respectively, for three reactions, which is much higher than that of the processes with the well-known TiO₂-based photocatalyst under UV light (1.5%).^{12,60} It should be noted that the yields reported here are approximations, as the absorption spectra shown include both absorption and scatter. As a consequence, the actual light absorption is lower than that derived from the absorption spectra, which means that the actual yields will be even higher than those we have estimated. This demonstrates that in these alloy NP structures the energy of incident light is very efficiently utilized to enhance the intrinsic catalytic activity of palladium.

Finally, the general concept that organic syntheses can be driven efficiently by sunlight at ambient temperatures with alloy NP catalysts composed of a plasmonic metal and a catalytically active transition metal is supported by the results presented here with Pd and Au.

4. CONCLUSIONS

The findings in the present study demonstrate that the intrinsic catalytic activity of Pd can be significantly enhanced at ambient temperatures by light irradiation of alloy Au–Pd NPs. In essence, this is because the charge heterogeneity of the alloy NP surface is greater than that of AuNP surface, leading to a stronger interaction between the alloy NPs and reactant molecules. The conduction electrons of the NPs gain the absorbed light energy, generating energetic conduction electrons at the surface Pd sites to which the reactant molecules have an affinity. The energetic electrons at the sites enhance their intrinsic catalytic ability to catalyze reactions. The Pd sites and the charge heterogeneity at the NP surface play key roles in the catalytic reactions. Because the distribution of Pd sites and charge heterogeneity at the NPs depends on the Au/Pd molar ratio, the ratio has an important influence on the catalytic performance of the alloy NPs. Because little input energy is consumed by other components of the reaction system, such as the solvent, support of the NPs, the atmosphere or container, this catalyst structure is highly efficient for driving various chemical reactions with sunlight. The knowledge acquired in this study may inspire further studies in new efficient catalysts

of gold and other transition metals for a wide range of organic syntheses driven by sunlight.

■ ASSOCIATED CONTENT

■ Supporting Information

Detailed data, schemes, and methods. This material is available free of charge via the Internet at <http://pubs.acs.org>.

■ AUTHOR INFORMATION

Corresponding Author

*E-mail: hy.zhu@qut.edu.au.

Notes

The authors declare no competing financial interest.

■ ACKNOWLEDGMENTS

The authors also gratefully acknowledge financial support from the Australia Research Council (ARC DP110104990).

■ REFERENCES

- (1) Hartings, M. R. *Nat. Chem.* **2012**, *4*, 764.
- (2) Seechurn, C. J.; Kitching, M. O.; Colacot, T. J.; Snieckus, V. *Angew. Chem., Int. Ed.* **2012**, *51*, 5062.
- (3) Stahl, S. S. *Science* **2005**, *309*, 1824.
- (4) Mulvaney, P. *Langmuir* **1996**, *12*, 788.
- (5) Eustis, S.; El-Sayed, M. A. *Chem. Soc. Rev.* **2006**, *35*, 209.
- (6) Liz-Marzán, L. M. *Langmuir* **2006**, *22*, 32.
- (7) Kamat, P. V. *J. Phys. Chem. B* **2002**, *106*, 7729.
- (8) Yamada, K.; Miyajima, K.; Mafun, F. *J. Phys. Chem. C* **2007**, *111*, 11246.
- (9) Link, S.; Burda, C.; Wang, Z. L.; El-Sayed, M. A. *J. Chem. Phys.* **1999**, *111*, 1255.
- (10) Voisin, C.; Del Fatti, N.; Christofilos, D.; Vallee, F. *J. Phys. Chem. B* **2001**, *105*, 2264.
- (11) Chen, X.; Zhu, H. Y.; Zhao, J. C.; Zheng, Z. F.; Gao, X. P. *Angew. Chem., Int. Ed.* **2008**, *47*, 5353.
- (12) Zhu, H. Y.; Ke, X. B.; Yang, X. Z.; Sarina, S.; Liu, H. W. *Angew. Chem., Int. Ed.* **2010**, *49*, 9657.
- (13) Zhu, H. Y.; Chen, X.; Zheng, Z. F.; Ke, X. B.; Jaatinen, E.; Zhao, J. C.; Guo, C.; Xie, T. F.; Wang, D. J. *Chem. Commun.* **2009**, 7524.
- (14) Kotsifa, A.; Halkides, T. I.; Kondarides, D. I.; Verykios, X. E. *Catal. Lett.* **2002**, *79*, 113.
- (15) Gao, F.; Wang, Y. L.; Goodman, D. W. *J. Phys. Chem. C* **2009**, *113*, 14993.
- (16) Zhang, H. J.; Watanabe, T.; Okumura, M.; Haruta, M.; Toshima, N. *Nat. Mater.* **2012**, *11*, 49.
- (17) Toshima, N.; Kanemaru, M.; Shiraiishi, Y.; Koga, Y. *J. Phys. Chem. B* **2005**, *109*, 16326.
- (18) Tang, W. J.; Henkelman, G. *J. Chem. Phys.* **2009**, *130*, 194504.
- (19) Chen, M. S.; Kumar, D.; Yi, C. W.; Goodman, D. W. *Science* **2005**, *310*, 291.
- (20) Link, S.; El-Sayed, M. A. *Int. Rev. Phys. Chem.* **2000**, *19*, 409.
- (21) Diederich, F.; Stang, P. J. *Metal-Catalyzed Cross-Coupling Reactions*; VCH: Weinheim, 1998.
- (22) Frisch, A. C.; Beller, M. *Angew. Chem., Int. Ed.* **2005**, *44*, 674.
- (23) Lang, X. J.; Ji, H. W.; Chen, C. C.; Ma, W. H.; Zhao, J. C. *Angew. Chem., Int. Ed.* **2011**, *50*, 3934.
- (24) Lang, X. J.; Ma, W. H.; Zhao, Y. B.; Chen, C. C.; Ji, H. W.; Zhao, J. C. *Chem.—Eur. J.* **2012**, *18*, 2624.
- (25) Zhu, B. L.; Lazar, M.; Trewyn, B. G.; Angelici, R. J. *J. Catal.* **2008**, *260*, 1.
- (26) Murahashi, S. I. *Angew. Chem., Int. Ed.* **1995**, *34*, 2443.
- (27) Samec, J. S. M.; Éll, A. H.; Backvall, J. E. *Chem.—Eur. J.* **2005**, *11*, 2327.
- (28) Grirrane, A.; Corma, A.; Garcia, H. *J. Catal.* **2009**, *264*, 138.
- (29) Landge, S. M.; Atanassova, V.; Thimmaiah, M.; Torok, B. *Tetrahedron Lett.* **2007**, *48*, 5161.
- (30) Neumann, R.; Levin, M. *J. Org. Chem.* **1991**, *56*, 5707.
- (31) Mallat, T.; Baiker, A. *Chem. Rev.* **2004**, *104*, 3037.
- (32) Sheldon, R. A.; Kochi, J. K. *Metal-Catalyzed Oxidations of Organic Compounds*; Academic Press: New York, 1981.
- (33) Hill, C. L. In *Advances in Oxygenated Processes*; Baumstark, A. L., Ed.; JAI Press: London, 1988; Vol. 1, p 1.
- (34) Hudlucky, M. *Oxidations in Organic Chemistry*, ACS Monograph Series; American Chemical Society: Washington, DC, 1990.
- (35) Comprehensi, V. In *Organic Synthesis*; Trost, B. M., Fleming, I., Eds.; Pergamon: Oxford, U.K., 1991.
- (36) Patel, K.; Kapoor, S.; Dave, D. P.; Mukherjee, T. *Res. Chem. Intermed.* **2006**, *32*, 103.
- (37) Lee, Y. W.; Kim, N. H.; Lee, K. Y.; Kwon, K.; Kim, M.; Han, S. W. *J. Phys. Chem. C* **2008**, *112*, 6717.
- (38) Chen, Y. H.; Tseng, Y. H.; Yeh, C. S. *J. Mater. Chem.* **2002**, *12*, 1419.
- (39) Emeline, A.; Kataeva, G. V.; Rudakova, A. S.; Ryabchuk, V. K.; Serpone, N. *Langmuir* **1998**, *14*, 5011.
- (40) Molnar, A. *Chem. Rev.* **2011**, *111*, 2251.
- (41) (a) So, M. H.; Liu, Y. G.; Ho, C. M.; Che, C. M. *Chem. Asian J.* **2009**, *4*, 1551. (b) Éll, A. H.; Samec, J. S. M.; Brasse, C.; Backvall, J.-E. *Chem. Commun.* **2002**, 1144.
- (42) Yamaguchi, K.; Mizuno, N. *Angew. Chem., Int. Ed.* **2003**, *42*, 1480.
- (43) Lang, X. J.; Ji, H. W.; Chen, C. C.; Ma, W. H.; Zhao, J. C. *Angew. Chem., Int. Ed.* **2011**, *123*, 4020.
- (44) Blackburn, T. F.; Schwartz, J. *J. Chem. Soc., Chem. Commun.* **1977**, 157.
- (45) Mori, K.; Hara, T.; Mizugaki, T.; Ebitani, K.; Kaneda, K. *J. Am. Chem. Soc.* **2004**, *126*, 10657.
- (46) Nishimura, T.; Kakiuchi, N.; Inoue, M.; Uemura, S. *Chem. Commun.* **2000**, 1245.
- (47) Dimitratos, N.; Villa, A.; Wang, D.; Porta, F.; Su, D.; Prati, L. *J. Catal.* **2006**, *244*, 113.
- (48) Liotta, L. F.; Venezia, A. M.; Deganello, G.; Longo, A.; Martorana, A.; Schay, Z.; Gucci, L. *Catal. Today* **2001**, *66*, 271.
- (49) Chen, J.; Zhang, Q.; Wang, Y.; Wan, H. *Adv. Synth. Catal.* **2008**, *350*, 453.
- (50) Choi, K.-M.; Akita, T.; Mizugaki, T.; Ebitani, K.; Kaneda, K. *New J. Chem.* **2003**, *27*, 324.
- (51) Uozumi, Y.; Nakao, R. *Angew. Chem., Int. Ed.* **2003**, *42*, 194.
- (52) Kesavan, L.; Tiruvalam, R.; Rahim, M. H. A.; Saiman, M. I. B.; Enache, D. I.; Jenkins, R. L.; Dimitratos, N.; Lopez-Sanchez, J. A.; Taylor, S. H.; Knight, D. W.; Kiely, C. J.; Hutchings, G. J. *Science* **2011**, *331*, 195.
- (53) Enache, D. I.; Edwards, J. K.; Landon, P.; Solsona-Espriu, B.; Carley, A. F.; Herzing, A. A.; Watanabe, M.; Christopher, J.; Kiely, C. J.; Knight, D. W.; Hutchings, G. J. *Science* **2006**, *311*, 362.
- (54) Ke, X. B.; Sarina, S.; Zhao, J.; Zhang, X. G.; Chang, J.; Zhu, H. Y. *Chem. Commun.* **2012**, 48, 3509.
- (55) Ke, X. B.; Zhang, X. G.; Zhao, J.; Sarina, S.; Barry, J.; Zhu, H. Y. *Green Chem.* **2013**, *15*, 236.
- (56) Fang, P. P.; Li, J. F.; Lin, X. D.; Anema, J. R.; Wu, D. Y.; Ren, B.; Tian, Z. Q. *J. Electroanal. Chem.* **2012**, *665*, 70.
- (57) Heugebaert, T. S. A.; Corte, S. D.; Sabbe, T.; Hennebel, T.; Verstraete, W.; Boon, N.; Stevens, C. V. *Tetrahedron Lett.* **2012**, *53*, 1410.
- (58) Conte, M.; Miyamura, H.; Kobayashi, S.; Chechik, V. *J. Am. Chem. Soc.* **2009**, *131*, 7189.
- (59) Maldotti, A.; Molinari, A.; Juarez, R.; Garcia, H. *Chem. Sci* **2011**, *2*, 1831.
- (60) Serpone, N. *J. Photochem. Photobiol., A* **1997**, *104*, 1.